J. Webster (ed.), *Wiley Encyclopedia of Electrical and Electronics Engineering*
Copyright © 1999 John Wiley & Sons, Inc.

COMPUTATIONAL MAGNETOSTATICS

Magnetism has one of the longest histories of any scientific application, beginning before 4000 B.C. to now. Accounts of early Chinese and European use of naturally occurring permanent magnetic material are reported in the classical text *De magnete*, written by the English scientist William Gilbert in 1600. However, until the beginning of the nineteenth century, the only improvement to applied magnetism was simply transferring the magnetic effect of existing magnetized lodestone to manufactured steel. At that time, compass needles were the primary application of permanent magnets, though marketing as a remedy for all known illnesses and complaints is also reported! The beginning of the era of electrical engineering is credited to Hans C. Oersted with his detection of the action of an electric current on a magnet needle in 1820. With this experiment, he showed the possibility of producing a magnetic influence from a source other than a permanent magnet. Since then, scientists such as C. F. Gauss, M. Faraday, and J. C. Maxwell developed the theory of electromagnetism by introducing the concept of electric and magnetic fields. Later, many electrical engineers invented a large variety of applications, from the needle telegraph to the hard disk drive of a computer.

The general feature of magnetic devices is the presence of a magnetic circuit energized by an electric circuit. A magnetic circuit is made of iron, since it is the only way to either give rise to important mechanical effects, as in electric motors, or to concentrate the magnetic flux lines for an efficient transmission of energy, as in transformers. An electric circuit is made of one or several copper windings or bars in which currents impressed by some generators flow. Figures 1(a) and 1(b) present two frequently occurring applications: a rotating machine and a single-phase transformer, respectively. In electric machines producing movement, such as actuators and electric motors, the electromagnetic principle is the conversion of energy between electromagnetic and mechanical forms. The mechanical force results from the action of a magnetic field on current-carrying conductors or on iron parts. In transformers, the governing phenomenon is the time variation of a magnetic flux generated by one side of the electric circuit, which allows the induction of electromotive force and currents in the other side. A full description of the physical behavior requires Maxwell's equations, which are partial differential equations. These equations are coordinate and time dependent and often nonlinear, so their treatment is very complex. Magnetostatics is an element of electromagnetic theory in which devices operate under steady-state conditions without any eddy-current phenomena. Although rare in electrical engineering, static analyses can lead to interesting practical results. This is so because at the low industrial frequencies (50 Hz to 60 Hz) the quasi static hypothesis is generally accepted. As a result, no propagation occurs and the magnetic field distribution causes no dynamic distortion unless induced currents are present.

Magnetic devices have traditionally been designed by combining empirical rules based on experimental evidence with simplified analytic models. As devices become increasingly varied and complex, however, conventional design rules are no longer adequate and the solution of electromagnetic field equations becomes necessary. The advent of the digital computer over the past three decades has triggered the development of numerical methods for solving the electromagnetic field equations. For the designer, these new computational tools provide more accurate solutions to problems than were previously possible. Moreover, computational electromagnetics enables efficient designs of devices, avoiding costly prototypes. All engineering field-oriented software now available uses the finite-element method. The principle is to subdivide the domains under study

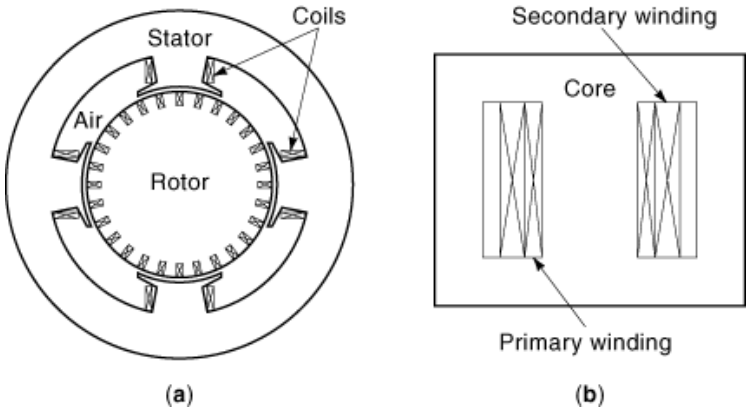

Fig. 1. (a) The magnetic circuit of a direct-current motor is made of two separate parts: the stator and the rotor. There are separate coils wound on each part. (b) A single-phase transformer is obtained by winding two coils, denoted as primary and secondary, around a unique magnetic circuit (core).

into a number of basic building blocks, or elements, for which the solution is approximated in a simple way, for instance, linearly. Then, Maxwell's equations are solved by using compatibility conditions between elements. Finally, a large system of algebraic equations results. The solution of this system gives a discrete approximation of the true solution to which the system should converge as the finite-element decomposition is refined. Although many analysis packages are reliable and effective, the various mathematical aspects of the finite-element method are still at the research level. The drive toward continuous improvement of software is demonstrated by the large attendance at specialized conferences and meetings on the topic (1). Numerical field computation has introduced the concept of optimization. The design variables are geometrical proportions, excitation parameters and material properties. Mathematically, optimization amounts to minimization of some function of those variables under constraint. In an iterative way, several field computations are carried out, converging to the optimized structure.

It is worth describing several important aspects of computer-aided design (*CAD*) in magnetics. First, preprocessing is the starting phase in which the problem to be solved is defined. Geometry, material property, excitations, and boundary conditions are discussed here. The finite-element decomposition or mesh also takes place in the preprocessor. The final product is an unambiguously defined mathematical problem ready for solution. Next, the solver builds the system of equations and produces its solution. This is the most time-consuming part and is often set up as batch process, since it generally does not require any interactive control by the user. In most magnetics problems, the end product of the solution program is a set of values of some indirect function describing the magnetic field in the entire problem space. These data provide raw information that is not usually what is required by the designer. Interesting engineering results are much more likely to include derived quantities such as inductances, forces, or flux density distributions. Then, further mathematical manipulation is implemented. This is the role of postprocessing, which provides the mathematical and graphical facilities for computing and displaying useful results. Those features are common in any *CAD* package and are designed to be effective in the hands of nonspecialist users. *CAD* techniques should not be used in a systematic way; they are rather complementary methods to traditional design.

The validation of the numerical methods involved in the various computer codes is made possible by using three kinds of benchmarks: (1) test examples with analytic solutions, (2) experimental results, and (3) numerical solutions obtained by other methods. The development of test examples adapted to specific electromagnetic problems is the goal of an international (Testing Electromagnetic Analysis Methods) workshop (*TEAM*). The

first meeting was held in 1986 at Argonne National Laboratory. The proposed problems are generally of simple shape in order to avoid any difficulty during the preprocessing operations.

This article outlines the mathematical modeling of magnetostatics starting from Maxwell's equations to useful integral formulation. Two-dimensional problems are first considered, since it is historically logical and because many industrial applications can be accurately analyzed in two dimensions. For instance, the study of the cross section of an electric machine is often sufficient for evaluating its main characteristics. Next, the finite-element method is presented. The computation of global quantities from field solutions is described because of their industrial interest. Technical advances and state-of-the-art procedures are summarized in the last section, where we have limited the presentation to such three-dimensional aspects as gauging problems, scalar potential alternatives, and edge elements. Indeed, the passage from two to three dimensions proved very difficult, since the form of equations is very different. Other problems, such as magnetic hysteresis, anisotropy, and optimization algorithms are also at the research forefront, but we merely mention them here.

Equations and Modeling

Maxwell's Equations. General electromagnetic field problems are governed by a set of equations derived by James C. Maxwell during the second part of the nineteenth century. These are partial differential equations that link electric and magnetic phenomena in space and time. In this article, we write the equations in the magnetostatic context

$$\text{curl } \boldsymbol{H} = \boldsymbol{J} \tag{1}$$

$$\text{div } \boldsymbol{B} = 0 \tag{2}$$

where $\boldsymbol{H}$ is the magnetic field [in ampere/meter (A/m)], $\boldsymbol{B}$ is the magnetic flux density [in teslas (T)] and $\boldsymbol{J}$ the current density [in ampere/meter^2 (A/m^2)]. The first equation is known as Ampere's law while the second is Gauss's law. In addition, we must add the constitutive relation

$$\boldsymbol{B} = \mu \boldsymbol{H} \tag{3}$$

where μ is the permeability [in henry/meter (H/m)] of the embedding medium. Recall that in free space, its value is $\mu_0 = 4\pi \times 10^{-7}$ H/m. The permeability is not always a simple constant. In the important case of ferromagnetic materials, the $\boldsymbol{B}$–$\boldsymbol{H}$ relationship is a nonlinear law called the magnetization curve, and in an anisotropic medium, it should be written as a tensor. The nonlinear case is discussed further later. The inverse of the permeability is called the reluctance $\nu = 1/\mu$.

Along the interface of two regions of different permeability the fields $\boldsymbol{B}$ and $\boldsymbol{H}$ are discontinuous as follows:

- The tangential component of $\boldsymbol{H}$ is discontinuous by an amount corresponding to any surface current density that may be present;
- The normal component of $\boldsymbol{B}$ is always continuous.

The direct computation of electromagnetic fields from Maxwell's equations is generally not feasible. For this purpose, fields must be represented by potential functions. Variables that allow nice formulations are easier to solve, either analytically or numerically. Many formulations exist depending on the type of problem.

A steady-state magnetic field is often described by the magnetic vector potential $\boldsymbol{A}$, which is very interesting for two-dimensional analysis.

Formulation with the Magnetic Vector Potential.

Definition. Equation (2) states that the divergence of $\boldsymbol{B}$ is zero. Therefore it can be expressed as the curl of a vector variable

$$\boldsymbol{B} = \operatorname{curl} \boldsymbol{A} \tag{4}$$

where $\boldsymbol{A}$ is called the magnetic vector potential. It is not unique, since we can add to it the gradient of any scalar function without violating Eq. (4). Then an extra condition must be imposed; it is generally expressed in terms of the divergence of $\boldsymbol{A}$. A usual choice is the Coulomb gauge, that is

$$\operatorname{div} \boldsymbol{A} = 0$$

By combining Eqs. (1), (3), and (4), we obtain

$$\operatorname{curl} (v \operatorname{curl} \boldsymbol{A}) = \boldsymbol{J} \tag{5}$$

which is the formulation of magnetostatics in terms of the magnetic vector potential. This equation holds true in the various domains of the problem under consideration. It must be solved together with the gauge condition and some boundary conditions in order to have a unique solution.

Two-Dimensional Magnetostatics. Although there is considerable practical interest in three-dimensional problems, a great majority of industrial cases tend to be handled by a two-dimensional approximation, as is the case for translational symmetry, that is, when cross-sectional geometry, excitation, and material properties remain unchanged along a given direction (say z). This hypothesis is generally accepted for structures that present a length dimension with respect to another dimension, such as transmission lines or rotating machines. In such cases the mathematical model is simplified, which results in substantial economy with respect to computing resources. Moreover, it often gives sufficiently accurate results even though the end effects are neglected. Henceforth, we consider problems stated in the Cartesian coordinate system (x, y, z) with its orthonormal vector basis ($\boldsymbol{u}_x, \boldsymbol{u}_y, \boldsymbol{u}_z$).

In two-dimensional problems, we suppose that the flux density has no component along the z direction, that is

$$\boldsymbol{B} = B_x \boldsymbol{u}_x + B_y \boldsymbol{u}_y$$

while the current density flows in the normal direction

$$\boldsymbol{J}_s = J_s \boldsymbol{u}_z$$

The magnetic vector potential $\boldsymbol{A}$ must have the same form as $\boldsymbol{J}$ in order to obtain $\boldsymbol{B}$ in the x–y plane

$$\boldsymbol{A} = A \boldsymbol{u}_z$$

Then, from Eq. (4), the components of $\boldsymbol{B}$ are found to be

$$B_x = +\frac{\partial A}{\partial y}, \qquad B_y = -\frac{\partial A}{\partial x} \tag{6}$$

A geometric interpretation of the vector potential in the two-dimensional case can now be derived. On the one hand, the change in A on moving from the point (x, y) to $(x + dx, y + dy)$ is

$$dA = \frac{\partial A}{\partial x} dx + \frac{\partial A}{\partial y} dy \tag{7}$$

On the other hand, if the displacement (dx, dy) is along a flux line, we have the proportionality relation.

$$\frac{dx}{B_x} = \frac{dy}{B_y}$$

If we combine Eqs. (6) and (7), dA vanishes, so that A remains constant along the flux lines. The flux distribution is then given by the equipotential contours of A. It is also readily seen that the condition $\boldsymbol{B} \times \mathbf{n} = 0$ is equivalent to $\partial A/\partial n = 0$.

Performing some differentiation, Eq. (5) reduces to the two-dimensional form

$$\operatorname{div}(\nu \operatorname{grad} A) = -J \tag{8}$$

This is the fundamental equation of two-dimensional magnetostatics. We note that the vector potential is automatically divergence free ($\operatorname{div} A = 0$), since it reduces to its z-component$A$, which only depends on x and y. Equation (8) fits the inhomogeneous Poisson equation, and some boundary conditions must be imposed in order to obtain a unique solution. There are two kinds of boundary conditions:

- *Dirichlet Condition*. A potential value is prescribed along a part of the boundary, it is the case of a symmetry flux line.
- *Neumann Condition*. The normal derivative $\partial A/\partial n$ vanishes along a plane of symmetry as at an iron surface with infinite permeability where flux lines emerge normally from the surface.

The interface conditions between two regions of different permeability μ_1 and μ_2 are stated as follows in terms of magnetic potential

$$A_1 = A_2$$
$$\nu_1 \frac{\partial A}{\partial n_1} = -\nu_2 \frac{\partial A}{\partial n_2}$$

These conditions are implicitly taken into account when solving Eq. (8). But some numerical schemes require them in an explicit form.

Finally, it is interesting to mention that problems with axial symmetry also allow a two-dimensional representation. In that case the cylindrical coordinate system (r, ϕ, z) is used, and there is an invariance with respect to ϕ. It can be shown that both current and vector potentials have only ϕ components while the flux density $\boldsymbol{B}$ is directed entirely in the (r, z) plane.

The Finite-Element Method

Two-dimensional (*2-D*) magnetostatics is completely described by Eq. (8) and some boundary conditions. However, an analytic solution is only available for structures of simple geometry. Industrial magnetic devices are

generally of complicated shape so that the fields and related global quantities can only be accurately computed numerically. The most commonly used technique in computer-aided design is the finite-element method, which has proved flexible, reliable, and effective. Although the method will be described in the context of *2-D* magnetostatics, the developed ideas are very general and can be transposed to any physical problem governed by partial differential equations.

The very first requirement of the finite-element method is to find an integral formulation equivalent to Eq. (8). In general, it consists of a relationship that contains integrals over the whole problem space and its boundary. Then the domain is subdivided into finite elements that are generated through, for instance, a triangular section. This is the discretization step. Next, a polynomial approximation of the potential A is chosen for each element. The higher the order of approximation, the better the accuracy, but for easy integration the order should not be excessive. Several orders are available for the triangular elements but only the first order will be considered in this presentation. The just noted treatment leads to the assembly of a system of algebraic equations that are a discrete equivalent of the original continuous formulation of the problem. The solution of this system is a finite set of potential values at each vertex of the triangular mesh. Finally, some postprocessing operations are carried out in order to obtain engineering results.

Weak Formulation. Consider a two-dimensional magnetostatic problem defined on a domain Ω of boundary Γ. Figure 2(a) presents the outline of a lifting magnet as an example. The domain Ω is piecewise homogeneous since the energizing coil is made of copper ($\mu = \mu_0$), the core and the plate are made of iron ($\mu \gg \mu_0$, say 1000), and the device is embedded in air ($\mu = \mu_0$). Phenomena are governed by the nonhomogeneous Poisson equation, [Eq. (8)], subject to the Dirichlet and Neumann boundary conditions on the parts Γ_A and Γ_q with $\Gamma = \Gamma_A \cup \Gamma_q$:

$$A = A_0 \text{ on } \Gamma_A, \quad \frac{\partial A}{\partial n} = 0 \text{ on } \Gamma_q$$

Figure 2(b) shows the boundary conditions for the considered example. On the one hand, the unbounded embedding air region is replaced by a rectangular box of suitable size for finite-element analysis. Its sides are assumed to be at zero magnetic vector potential. This hardly perturbs the local field near the magnet poles. On the other hand, the problem space of our example is reduced to one-half its size by exploiting the obvious mirror symmetry.

We now define the following quantity, called the residual,

$$R(A) = \text{div } \nu \text{ grad } A + J$$

which vanishes for the exact solution A of the problem. Distribution theory shows that the differential formulation of the problem is equivalent to finding the variable A that verifies the integral statement.

$$\int_\Omega R(A) w d\Omega = 0$$

that is,

$$\int_\Omega w \text{ div } \nu \text{ grad } A \, d\Omega = -\int_\Omega w J \, d\Omega \qquad (9)$$

where w is any weighting or test function. Equation (9) gives the starting point of the weighted residual procedure for deriving the integral formulation exploited in the finite- element method.

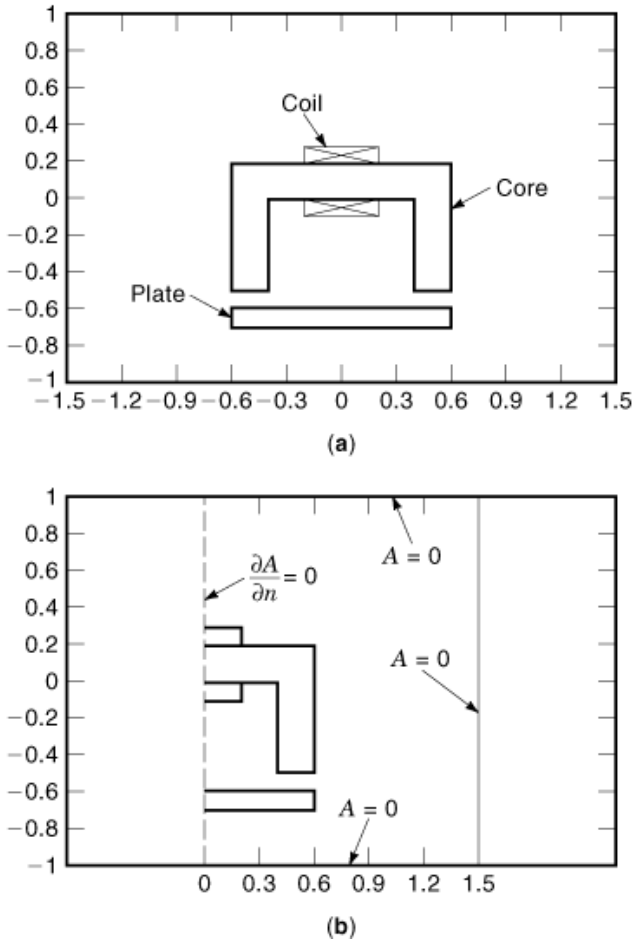

Fig. 2. Example of a two-dimensional magnetostatic problem: a lifting magnet. (a) Outline of the problem space with dimensions in meters. (b) Half the geometry with the related boundary conditions. There are five domains in this problem.

The left-hand side of Eq. (9) can be transformed by performing some integration by parts. If we apply the differentiation rule,

$$\operatorname{div} f\boldsymbol{G} = f \operatorname{div} \boldsymbol{G} + \boldsymbol{G} \cdot \operatorname{grad} f$$

we obtain

$$-\int_\Omega \upsilon \operatorname{grad} w \cdot \operatorname{grad} A \, d\Omega + \int_\Omega \operatorname{div} (w\upsilon \operatorname{grad} A) \, d\Omega = -\int_\Omega wJ \, d\Omega$$

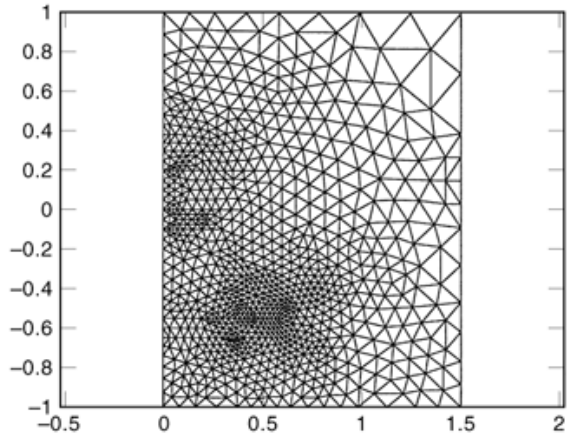

Fig. 3. Discretization of the domains. Delaunay's algorithm is usually used due to its good triangle conditioning. The regions where the potential may have sharp variations are automatically finely meshed.

with the application of the divergence theorem to the second integral on the left, a boundary integral appears:

$$-\int_\Omega v\ \text{grad}\ w \cdot \text{grad}\ A\, d\Omega + \oint_\Gamma vw \frac{\partial A}{\partial n} d\Gamma = -\int_\Omega wJ\, d\Omega \quad (10)$$

where $\boldsymbol{n}$ is the outward normal to the boundary Γ. This integral may be split into two contributions in accordance with the subdivision of Γ. The integral on Γ_q vanishes because of the Neumann condition and so does the integral on Γ_A if we choose $w = 0$ on this part.

The integral formulation we sought is given by Eq. (10), where the boundary integral is eliminated. Finally, the two-dimensional magnetostatic problem is stated as: Find the function $A(x, y)$ such that $A = A_0$ on Γ_A and

$$\int_\Omega v\ \text{grad}\ A \cdot \text{grad}\ w\, d\Omega = \int_\Omega wJ\, d\Omega \qquad (11)$$

for all w such that $w = 0$ on Γ_A. Equation (11) is called a weak formulation in the sense that the order of the derivatives on A has been decreased or "weakened." This feature is important for the numerical treatment since the derived approximation of A does not need to verify the derivability constraints of the true solution. We will clarify this point later.

Finite Elements and Node Approximation. As stated previously, the next step is the discretization of the domain together with an approximation of the unknown function A. First-order triangular finite elements will be discussed here despite their relatively low accuracy. They have been supplanted by higher-order elements but they are still employed because of their ease of implementation.

Consider a triangular section of the domain Ω as depicted in Fig. 3. The obvious requirements of the mesh are that no overlapping element should occur and the discretization should cover the whole domain without any hole. Evidently, the boundary may be truncated owing to its possible curvature. In the following we

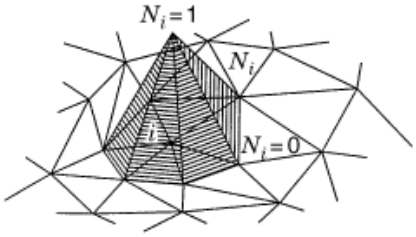

Fig. 4. Function N_i is made of planes above each triangle having node i in common and is zero everywhere.

call $\hat{\Omega}$ the mesh of the domain and $\hat{\Gamma}_A$ the mesh of Γ_A. The number of nodes of $\hat{\Omega}$ is n and n_x for $\hat{\Omega}/\hat{\Gamma}_A$. Thus $\hat{\Gamma}_A$ presents $n - n_x = n_0$ nodes. There are m elements Ω_e in Ω.

The function A is now replaced by a node approximation $\hat{A}$ that has the form

$$\hat{A} = N_1(x, y)\hat{A}_1 + N_2(x, y)\hat{A}_2 + \cdots + N_n(x, y)\hat{A}_n \qquad (12)$$

where the parameters $\hat{A}_i$ are the nodal values of the $\hat{A}$ and the N_i's are polynomial functions of first order that are called expansion or shape functions. Function $N_i = 1$ at node i and 0 at the others. Moreover, it must be linear on each element. The geometric aspect of N_i is depicted in Fig. 4. Consider a triangular element Ω_e defined by the vertices i, j, k; the local expression of N_i in x–y terms on this element is

$$N_i(x, y) = \frac{1}{2S_e}[(x_j y_k - x_k y_j) + (y_j - y_k)x + (x_k - x_j)y] \quad (13)$$

where S_e represents the surface area of the triangle. The remaining functions N_j and N_k can be obtained by permutation of subscripts.

Thus, the true smoothly curved solution A has been replaced by the piecewise-planar function $\hat{A}$, which is then a jewel-faceted approximation. The potential along any triangle edge is the linear interpolation between its two vertex values. That is to say, the potential approximation $\hat{A}$ will be continuous across any interelement boundary, and there are no gaps in the surface $\hat{A}(x, y)$. Owing to the piecewise-planar feature and the continuity of the approximation, it is expected that the first partial derivatives exist but the second ones are undefined. The weak formulation, Eq. (11), is then well fitted to the node approximation, Eq. (12), in the context of a numerical scheme.

Galerkin's Method. Returning to the integral formulation of two-dimensional magnetostatics, we have to solve Eq. (11) on the mesh Ω for a solution of the form in Eq. (12). Recall that there are n_x unknown parameters $\hat{A}_i$ to be found so that a set of n_x independent test functions has to be adopted in order to obtain the correct number of equations. The n_x functions N_i associated with the nodes of unknown potential values is a natural choice. It gives rise to the so-called Galerkin method. The continuous problem, Eq. (11), then becomes the following numerical scheme: Find the function $\hat{A}(x, y)$ of the form, Eq. (12), such that $\hat{A} = A_0$ on Γ_A and

$$\int_{\hat{\Omega}} \nu \, \mathrm{grad}\hat{A} \cdot \mathrm{grad}\, N_i \, d\Omega = \int_{\hat{\Omega}} N_i J \, d\Omega \qquad (14)$$

for any node i of $\hat{\Omega}_{\mathrm{h}}\hat{\Gamma}_A$. If $\hat{A}$ is replaced by its expression, Eq. (12), in eq. (14), we obtain

$$\sum_{k=1}^{n}\left(\int_{\hat{\Omega}} \nu \,\mathrm{grad}\, N_i \cdot \mathrm{grad}\, N_k \, d\Omega\right)\hat{A}_k = \int_{\hat{\Omega}} N_i J \, d\Omega \qquad (15)$$

Denoting the integrals under the summation by s_{ik} and the integrals on the right-hand side by f_i and writing Eq. (15) for each of the n_x function N_{i} as stated above, we set up the following system of algebriac equations

$$\begin{bmatrix} s_{11} & \cdots & s_{1n} \\ & \ddots & \\ s_{n_x 1} & \cdots & s_{n_x n} \end{bmatrix} \begin{bmatrix} \hat{A}_1 \\ \vdots \\ \hat{A}_n \end{bmatrix} = \begin{bmatrix} f_1 \\ \vdots \\ f_{n_x} \end{bmatrix}$$

or

$$(\boldsymbol{S} \qquad \boldsymbol{S}_0)\begin{pmatrix} \boldsymbol{A}_x \\ \boldsymbol{A}_0 \end{pmatrix} = \boldsymbol{f} \qquad (16)$$

where $\boldsymbol{S}$ and $\boldsymbol{S}_0$ are matrices of order $n_x \times n_x$ and $n_{\mathrm{s}} \times n_0$ respectively; $\boldsymbol{A}_x$ and $\boldsymbol{A}_0$ are, respectively, the vectors of the n_x unknown and n_0 prescribed nodal potentials assuming a suitable numbering of the nodes; and $\boldsymbol{f}$ is the source term (of order n_{x}).

Rearranging the system of equations, Eq. (16), by passing the unknowns to the left, we obtain the final regular system

$$\boldsymbol{S}\,\boldsymbol{A}_x = \boldsymbol{b} \qquad (17)$$

where $\boldsymbol{S}$ is the so-called stiffness matrix. Vector $\boldsymbol{b}$ results from the contribution of the excitation and the Dirichlet condition.

Assembling and Solving the Linear System. The practical assembly of the linear system, Eq. (17), requires another form for the expression in Eq. (15). Indeed, the domain Ω? is made up of triangular elements Ω_e with vertices i, j, k such that the integrals of the left-hand side have to be computed one triangle at a time. Therefore, we rewrite Eq. (15) as

$$\sum_{e}\sum_{p=i,\,j,\,k}\left(\int_{\Omega_e} \nu_e \,\mathrm{grad}\, N_i \cdot \mathrm{grad}\, N_p \, d\Omega\right)\hat{A}_p = \sum_{e}\int_{\Omega_e} N_i J \, d\Omega \qquad (18)$$

Each finite element gives rise to $3 \times 3 = 9$ entries in the global matrix of the system, Eq. (17). They are located at the rows and columns of indices *i, j, k.* The contribution of each triangular element

may be written out, as

$$\int_{\Omega_e}^{V_e} \begin{bmatrix} \left(\frac{\partial N_i}{\partial x}\frac{\partial N_i}{\partial x}+\frac{\partial N_i}{\partial y}\frac{\partial N_i}{\partial y}\right)\left(\frac{\partial N_i}{\partial x}\frac{\partial N_j}{\partial x}+\frac{\partial N_i}{\partial y}\frac{\partial N_j}{\partial y}\right) & \left(\frac{\partial N_i}{\partial x}\frac{\partial N_k}{\partial x}+\frac{\partial N_i}{\partial y}\frac{\partial N_k}{\partial y}\right) \\ \left(\frac{\partial N_j}{\partial x}\frac{\partial N_i}{\partial x}+\frac{\partial N_j}{\partial y}\frac{\partial N_i}{\partial y}\right)\left(\frac{\partial N_j}{\partial x}\frac{\partial N_j}{\partial x}+\frac{\partial N_j}{\partial y}\frac{\partial N_j}{\partial y}\right) & \left(\frac{\partial N_j}{\partial x}\frac{\partial N_k}{\partial x}+\frac{\partial N_j}{\partial y}\frac{\partial N_k}{\partial y}\right) \\ \left(\frac{\partial N_k}{\partial x}\frac{\partial N_i}{\partial x}+\frac{\partial N_k}{\partial y}\frac{\partial N_i}{\partial y}\right)\left(\frac{\partial N_k}{\partial x}\frac{\partial N_j}{\partial x}+\frac{\partial N_k}{\partial y}\frac{\partial N_j}{\partial y}\right) & \left(\frac{\partial N_k}{\partial x}\frac{\partial N_k}{\partial x}+\frac{\partial N_k}{\partial y}\frac{\partial N_k}{\partial y}\right) \end{bmatrix} \begin{bmatrix} \hat{A}_i \\ \hat{A}_j \\ \hat{A}_k \end{bmatrix} d\Omega \tag{19}$$

where the partial derivatives are readily derived from Eqs. (13):

$$\frac{\partial N_i}{\partial x} = \frac{1}{2S_e}(y_j - y_k), \qquad \frac{\partial N_i}{\partial y} = \frac{1}{2S_e}(x_k - x_j)$$

These are constant values so that the integrals of Eq. (19) are readily carried out. Finally, the matrix is built up iteratively by cumulation of the partial results of every triangle.

The current density is constant over each triangle so that the right-hand integrals of Eq. (18) reduce to the integration of the expansion functions over the elements. Geometrically, they measure the volume of a tetrahedron of unit height over a triangle of surface area S_e. We then have the result

$$\int_{\Omega_e} J \begin{bmatrix} N_i \\ N_j \\ N_k \end{bmatrix} d\Omega = J\frac{S_e}{3}\begin{bmatrix} 1 \\ 1 \\ 1 \end{bmatrix}$$

The linear system, Eq. (17), represents a discrete equivalent formulation of the original continuous problem, Eq. (11). The task of solving this system is not trivial, since it takes up a significant part of the total computation time. An important feature of finite elements is that they generally produce a very large number of equations, particularly in the treatment of industrial cases. Two-dimensional problems may lead to matrix equations with 1000 to 10,000 variables, while three-dimensional complicated geometric structures may require as many as 10,000 to 300,000 degrees of freedom. Fortunately, such systems are very sparse. Indeed, the expanded functions are defined locally over the mesh as illustrated in Fig. 4. Hence, from Eq. (12), we deduce that the only triangles having the node i in common produce a nonzero entry at row i in the global matrix. This feature determines the choice of the solution method of the linear system, and the storage of the coefficient matrix must take care of this structure. Moreover, in the magnetostatic case, the stiffness

matrix $\boldsymbol{S}$ is symmetric and positive definite. The solution methods are mainly of two types: the direct methods and the iterative methods. The direct techniques used in finite-element analysis programs are one or another version of the very popular Gaussian triangular decomposition algorithm. Until recently, they were preferred to iterative techniques because of their robustness and predictable behavior. But lately many researchers have discovered efficient iterative algorithms so that a rapid shift toward these new methods is now observed. The iterative techniques are faster and they are almost mandatory for the solution of large industrial problems. The preconditioned conjugate gradient method is now widely used in the area of computational electromagnetics. We do not go further in this global description, and the interested reader can find more details in Ref. 2.

Nonlinear Problems

Most magnetostatic problems involve the presence of iron and the magnetization curve has to be taken into account in order to obtain accurate engineering results. Then the reluctivity v is field dependent so that the system of algebraic equations, Eq. (16), is nonlinear. We rewrite this system in nonlinear form

$$\boldsymbol{K}(A)\,\boldsymbol{A} = \boldsymbol{f} \tag{20}$$

where $\boldsymbol{K}$ denotes the rectangular matrix ($\boldsymbol{S} \quad \boldsymbol{S}_0$). Matrix coefficients of $\boldsymbol{K}$ are now functions of the potential A through the reluctivity. The right-hand source vector $\boldsymbol{f}$ remains constant, since it does not depend on v. The nonlinearities encountered in magnetic problems are usually single-valued and can be assumed to be monotonic so that simple nonlinear computational methods can be used. The most commonly used method is the Newton–Raphson iteration process owing to its stability and fast convergence.

The Newton–Raphson iterative technique is based on the expansion of the product $\boldsymbol{K}(\boldsymbol{A})\cdot\boldsymbol{A}$ in a Taylor's series, where the terms are neglected beyond the second-order derivatives. For simplicity, the one-variable case is first discussed. Adapting notation, Eq. (20) becomes

$$K(a)a = P(a) = f \tag{21}$$

Let a_{ex} be the true solution and a^0 a nearby value; then the Taylor's series near a^0 is

$$P(a_{\text{ex}}) = f \simeq P(a^0) + \left.\frac{dP}{da}\right|_{a^0} \Delta a$$

or

$$-[P(a^0) - f] \simeq \left.\frac{dP}{da}\right|_{a^0} \Delta a \tag{22}$$

where we write the deviation $\Delta a = a_{\text{ex}} - a^0$. Now, the solution of Eq. (22) gives a value of Δa no longer equal to $a_{\text{ex}} - a^0$ because of the neglected terms, but it is easily understood that $a^1 = a^0 + \Delta a$ is nearer to a_{ex} than a^0. We say that a^1 is a better estimate for a_{ex}.

The Newton–Raphson iterative scheme is derived from this consideration and may be set up as follows:

$$\begin{aligned} -[P(a^n) - f] &= \left.\frac{dP}{da}\right|_{a^n} \Delta a^n \\ a^{n+1} &= a^n + \Delta a^n \end{aligned} \tag{23}$$

The process can be started by assuming an initi estimate of the true solution and it c be terminated when two successive solutions agree within some prescribed tolerance.

Nonlinear magnetostatics is the multidimensional extension of Eq. (23). It can be immediately deduced that

$$\boldsymbol{K}_{\mathrm{T}}^{n}\triangle\boldsymbol{A}^{n} = -[\boldsymbol{K}(A^{n})\boldsymbol{A}^{n} - f]$$
$$\boldsymbol{A}^{n+1} = \boldsymbol{A}^{n} + \triangle\boldsymbol{A}^{n}$$

where $\boldsymbol{K}_{\mathrm{T}}$ is the Jacobian matrix of the product $\boldsymbol{K}(\boldsymbol{A})\cdot\boldsymbol{A}$ and is called the tangent matrix. By performing some algebra, the matrix coefficient $\boldsymbol{k}_{\mathrm{T},ij}$ is derived as follows (we omit the superscript n for the sake of clarity):

$$k_{\mathrm{T}_{ij}} = \frac{\partial}{\partial A_j}[\boldsymbol{K}(A)\cdot\boldsymbol{A}]_i$$
$$= k_{ij}(A) + \sum_l A_l \frac{\partial k_{il}(A)}{\partial A_j}$$

From the detailed expression of k_{il},

$$k_{il}(A) = \int_{\hat{\Omega}} \upsilon(A)\,\mathrm{grad}\ N_i \cdot \mathrm{grad}\ N_l\, d\Omega$$

and introducing the flux density squared as a new variable, the chain rule of differentiation leads to the final result,

$$k_{\mathrm{T}_{ij}} = k_{ij} + 2\int_{\hat{\Omega}} \frac{d\upsilon}{dB^2}\left(\sum_p \mathrm{grad}\ N_i \cdot \mathrm{grad}\ N_p A_p\right)\left(\sum_q \mathrm{grad}\ N_j \cdot \mathrm{grad}\ N_q A_q\right) d\Omega \qquad (24)$$

which can be easily evaluated in the case of a section with first-order triangles. It is easily verified that the matrix structure of $\boldsymbol{K}_{\mathrm{T}}$ is exactly the same as that of $\boldsymbol{K}$ so that the treatment of a nonlinear problem imposes the same memory requirements as in the similar linear case. Equation (24) requires the magnetization curve to be modeled in the form $\upsilon = \upsilon(B^2)$. There exists a large panel of mathematical functions for modeling the magnetic characteristic of soft iron. Polynomial, exponential, rational algebraic, and various other functions have been employed for this purpose. However, for economy, it is best to avoid the use of transcendental functions, which usually entail a substantial computing cost. Note that slope continuity is desirable for smooth convergence in the Newton–Raphson process.

The convergence rate of the method is theoretically quadratic near the solution point, that is, the number of significant digits in each iterative trial solution should be approximately double the number of significant digits in the preceding one. In practice, more than seven or eight Newton–Raphson steps are rarely required to achieve levels of precision that exceed those that are physically justifiable. Acceleration techniques can also be used in order to improve the convergence as, for example, by calculating the Jacobian matrix for only the first iterations where the matrix is strongly changed (3).

Postprocessing Operations

The numerical solution of two-dimensional magnetostatic problems leads to the distribution of vector potential $\boldsymbol{A}$ over the whole problem space. This is not very interesting in itself for engineering purposes. But many relevant data meaningful for the practical user can be extracted from this field solution. This requires some operations that are generally termed postprocessing. There are two categories of engineering results: local values and global values. The first involve local field values such as the flux density $\boldsymbol{B}$ or the magnetic field $\boldsymbol{H}$. The local phenomena are of prime interest in many applications such as the magnetic recording head design. But global output values, rather than the details of the magnetic field distribution, are the final aim of most computer calculations in electric machine design. The most important values are force, torque, power, terminal impedance, and voltage. Reference 4 gives a good survey of the topic.

Local Field Values. The determination of fields and field gradients as local values or global distributions is important for the engineering designer. For example, the analysis of a recording head requires the computation of fields at specific points of the structure or the flux plot in the gap between the head and the recording area. Indeed, an important specification is that the magnetization of the recording medium must be high enough at the writing point but considerably lower elsewhere to avoid destroying information already recorded. Then, if the local values prove more or less satisfactory, the designer may well attempt to modify the shape of the head. In the case of rotating electric machines, the radial component of flux density in the air gap gives both a qualitative and quantitative indication of the coupling across the machine and may be used in the calculation of thrust and torque exerted on the shaft.

Most two-dimensional *CAD* systems employ the vector potential to represent magnetic events, so we take this variable to express the field values. We know from Eq. (6) that the flux density $\boldsymbol{B}$ can be computed easily by differentiation of the vector potential. The magnetic field $\boldsymbol{H}$ is then readily obtained. It was also pointed out that the equipotential contours of A directly give the plot of the flux lines. There are a great number of elegant methods for the visualization of field behavior. Contour plots or maps are the most commonly requested. The flux density vector distribution can be represented by a geometric image consisting of a properly scaled assembly of arrows. Assorted colors and gray shades are also frequently used to display field quantities. Some applications may require specific representations such as the graphic plot of a given field component against a given distance.

It should be kept in mind that we start from a set of approximate values of a potential function that is interpolated between the discretization points. Then, the piecewise continuity of the potential results in gradient distributions that are not smooth. In the case of a linear approximation on a triangular mesh, the flux density is piecewise constant on each element. The displays then appear ragged. It is possible to make the results more attractive by some interpolative smoothing, but it does not improve the accuracy.

Inductance Calculation. Suppose an inductor is energized by a dc current i. Let ϕ be the total magnetic flux linkage of the winding; the inductance L of the circuit is defined by

$$L = \phi / i$$

We now look for the expression of L in terms of the vector potential for a rectangular single-turn filamentary coil of infinite extension along one direction (say z). From the rules of vector differential calculus, the flux linked by this turn can be expressed as

$$\begin{aligned} \phi &= \int_S \boldsymbol{B} \cdot \boldsymbol{n}\, dS \\ &= \int_S \operatorname{rot} \boldsymbol{A} \cdot \boldsymbol{n}\, dS = \oint_C \boldsymbol{A}\, ds \end{aligned} \tag{25}$$

where C is the closed contour formed by the coil. Clearly, the problem is essentially two-dimensional so that the end contribution to the integral, Eq. (25), may be ignored. Along the two sides 1 and 2 parallel to the z axis, the vector potential has constant values A_1 and A_2. Then, Eq. (25) reduces to the simple result (per unit length)

$$\phi = A_2 - A_1$$

For the coil made of n tightly packed turns, the total flux linkage ϕ is n times larger than that in the single-turn coil given previously, that is,

$$\phi = n(A_2 - A_1)$$

Finally, the inductance of a thin multiturn coil is calculated as

$$L = \frac{n(A_2 - A_1)}{i} \tag{26}$$

When the winding fills an extended portion of space, there is no particular point at which to measure the vector potential. Equation (26) cannot be used as such and further mathematical development must be carried out. We merely give the final result:

$$L = \frac{1}{i^2} \int_S AJ \, dS$$

This expression shows that thickening the coil sides leads to forming some sort of average value of the vector potential weighted by the current density.

Force Calculation. ny magnetic devices such as actuators and electric motors are used to convert energy between electrical and mechanical forms. The evaluation of force and torque produced is then a common requirement in computer-aided design systems based on the finite-element technique. Two traditional methods exist for the calculation of electromagnetic forces and torques: the virtual work principle and the method of Maxwell stresses.

The Virtual Work Principle. First of all, recall that the magnetic energy W of a system made of current-carrying conductors and magnetized iron domains is defined as the work involved in forming this system from the quiescent state ($H = 0, B = 0$):

$$W = \int_\Omega \int_0^B H(B) \, dB \, d\Omega$$

A complementary quantity is necessary for the definition of force, namely, the magnetic coenergy W' of the system that is given by

$$\begin{aligned} W' &= \int_\Omega \int_0^H B(H) \, dH \, d\Omega \\ &= \int_\Omega HB \, d\Omega - \int_\Omega \int_0^B H(B) \, dB \, d\Omega \end{aligned}$$

Energy and coenergy are equal for linear material, but in the nonlinear case, they are not. Finally, the force F exerted on a body in an electromechanical system along a direction x may be calculated from the rate of change of coenergy with respect to x, while keeping the total current constant:

$$F = \left.\frac{\partial W'}{\partial x}\right|_i \tag{27}$$

In the same way, the torque is calculated from the rate of change of coenergy with respect to angular displacement (say θ):

$$T = \left.\frac{\partial W'}{\partial \theta}\right|_i \tag{28}$$

Equations (27) and (28) are known as the virtual work principle.

When combined with finite-element analysis, the derivatives have to be replaced by numerical differentiation. The energy is evaluated for the device under study in two positions separated by a small displacement. The same current is imposed for both positions. Then the difference in energy divided by the distance will give the value for the force. Let x_1 and x_2 be two successive positions along the x axis and W'_1 and W'_2 the related coenergy values; then Eq. (27) becomes

$$F \simeq \frac{W'_2 - W'_1}{x_2 - x_1}$$

A major inherent drawback of the method is that inaccurate results may arise for very small displacements. Then, the coenergies $W_{1'}$ and $W_{2'}$ are not very different, and there are as many significant figures lost in the subtraction as there are similar leading digits in both quantities. Some improvements are obtained by computing several points along the displacement vector instead of only at the two ends. The application of Eq. (27) to a smooth curve fitted to the obtained values leads to better results. A significant development in force computation evolves with an elegant scheme for implementing the virtual work principle without the need for several solutions. It employs the fact at the finite-element solutions are functions of space as given by the trial functions and are not just thexplicit nodal values that are returned. Using this, the energy W or the coenergy W' is evaluated as a function of the nodal values and spatial coordinates. Then it is differentiated analytically before the integration over the solution space is performed to eliminate the x and y coordinates. The results obtained through this scheme are more accute than those by other methods since it makes use of the explicit expression of energy, which is highly accurate in finite-element analysis (5).

Maxwell Stress Tensor. The most successful and straightforward technique for the finite-element force calculation is the method of Maxwell stresses. Basically, the method involves computing the magnetic stresses present on an imaginary closed contour C (a surface in three-dimensional problems) that is situated in the air space of a problem. The integration of these stresses over the contour results in the net force transmitted by the magnetic field. For a contour with normal flux density B_n and tangential flux density B_t the normal and tangential magnetic stresses σ and τ are given by, respectively,

$$\sigma = \frac{1}{2\mu_0}(B_\mathrm{n}^2 - B_\mathrm{t}^2), \qquad \tau = \frac{1}{\mu_0} B_\mathrm{n} B_\mathrm{t}$$

By integrating the stresses over the contour C and rearranging terms, the force acting on a body may be expressed as follows:

$$\boldsymbol{F} = \int_C \left(\frac{1}{\mu_0} \boldsymbol{B}(\boldsymbol{B} \cdot \boldsymbol{n}) - \frac{1}{2\mu_0} B^2 \boldsymbol{n} \right) ds$$

In principle, the contour C should be the contour of the body itself. But it is often more convenient to place C in the air surrounding the object. Anyway, the piece of air therewith attached to the rigid body carries no currents and has no magnetic properties. Numerical investigations in the Maxwell stress approach show that the results are very sensitive to discretization density and integration contour position (6). This is due to the very high irregularity of the B_t component. A remedy is to locate the integration contour as far as possible from iron parts; it should not lie on lines dividing layers of finite elements. It is also advisable to evaluate the force using several contours and then to average the results.

Modeling of the Rotation. The study of electric machines often requires analyses with rotation. Classically, three methods are usually used in two dimensions: the slip-line, the movement-band, and the macro-element techniques.

In the slip-line method, a line is defined in the middle of the air gap, which requires a regular mesh. The rotor displacement is modeled by a circular permutation of the unknowns according to the step mesh. With this approach, the displacement is limited by the step of the mesh.

The movement-band technique is based on the deformation of the elements in an area situated also in the middle of the air gap. When the deformation becomes very important, the band is remeshed by circular permutation. Thus the inherent limitation of the previous method is avoided.

Finally, the macro-element method consists in solving analytically the Laplace equation in a regular band situated in the same area as the movement band. Such an element permits armature rotation without changing the nodal coordinates (7). Moreover, there is no limitation to the displacement. However, the computation time is increased compared with the preceding techniques.

Example

The finite-element analysis of a problem may be illustrated by a simple two-dimensional magnetostatic example. It relates to the lifting magnet already shown in Fig. 2(a). A current density J of 1 A/mm^2 flows through the exciting coil, and the relative permeability of the iron (core and plate) is 1000. The related boundary conditions are given in Fig. 2(b).

Thproblem is triangulated as displayed in Fig. 3. The mesh includes 926 nodes and 1780 triangles. By subtracting the nodes with prescribed potential, there are 889 degrees of freedom in the analysis. Note that the mesh is adapted to the normally expected solution; many small elements are employed in which the potential presents sharp fluctuations, while relatively coarse elements are sufficient elsewhere. The mesh may be refined or adapted after a first calculation.

Equipotential lines are depicted in Fig. 5. The flux density is displayed in the form of gray shades and arrow distributions in Fig. 6 and 7, respectively.

Three-Dimensional Magnetostatics

The Magnetic Vector Potential Approach. The fundamentals presented in the previous sections are of frequent use in computational magnetostatics, since a two-dimensional analysis is sufficient in many industrial applications. However, in order to answer new practical questions of designers, there is an increasing need for full three-dimensional analyses. These imply larger computing times and the manipulation of vast

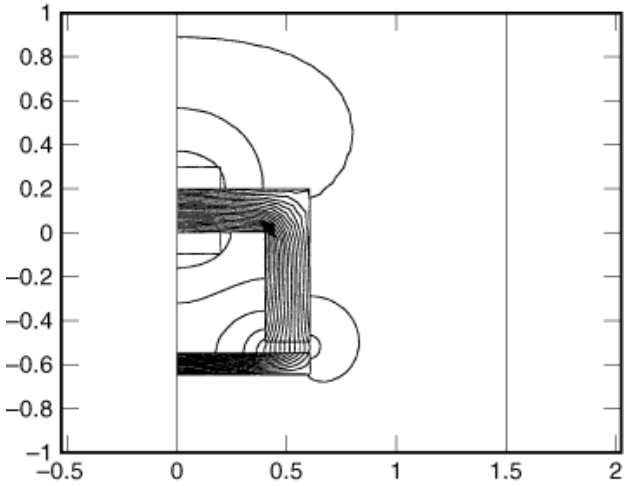

Fig. 5. Equipotential lines of the lifting magnet example. These are also the flux lines. Note they nearly impinge at right angles at the air–iron interface due to the high discontinuity in the permeability of both regions.

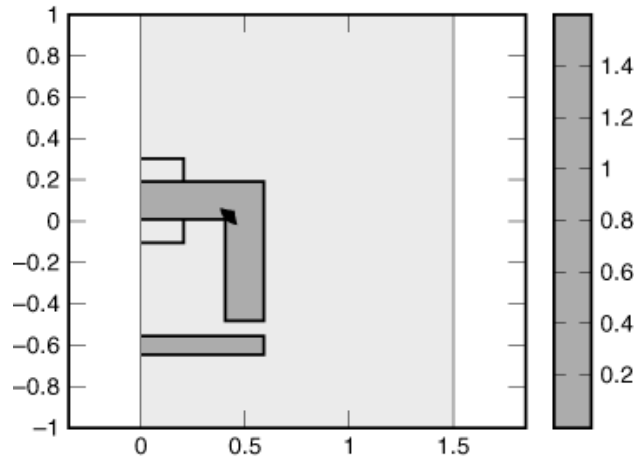

Fig. 6. Intensity plot of flux density by using gray shades (B in teslas). Each triangle has a constant gray level because of the linear approximation of vector potential.

quantities of data in both the preprocessing (geometry description, discretization) and postprocessing (visualization of the results) operations. However the problem instead lies in the mathematical formulation. Indeed, the application of the magnetic vector potential to two-dimensional problems is straightforward, since it reduces to a scalar quantity uniquely defined by a Poisson-type differential equation. This is not the case in the general three-dimensional situation, so we face three degrees of freedom per node instead of one. Nevertheless, this fact becomes less and less important with the development of increasingly faster computers. The real problem lies in the nonuniqueness of the vector potential unless a gauge condition is defined. This has been a subject of discussion for many years and we give below the main results.

Recall that the general magnetostatic problem defined on a domain Ω is governed by the curl–curl equation (5) completed with specified conditions $\boldsymbol{B}\cdot\boldsymbol{n} = 0$ and $\boldsymbol{H} \times \boldsymbol{n} = 0$ on the complementary parts of the boundary.

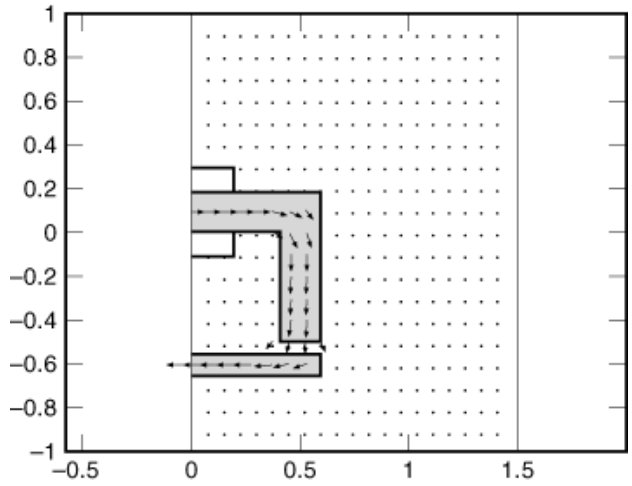

Fig. 7. Flux distribution with arrows in a Cartesian grid.

The related weak integral formulation is derived in the same way as for the Poisson problem, that is,

$$\int_\Omega v \operatorname{curl} \boldsymbol{A} \cdot \operatorname{curl} \boldsymbol{A}' \, d\Omega = \int_\Omega \boldsymbol{A}' \cdot \boldsymbol{J} \, d\Omega \qquad (29)$$

where $\boldsymbol{A}'$ is a vector test function that vanishes on the boundary $\boldsymbol{B} \cdot \boldsymbol{n} = 0$. Therefore, this formulation can be discretized by the classical finite-element technique. The solution of Eq. (29) is unique provided a gauge condition is enforced. Alternative gauges are possible. As said before, the Coulomb gauge (div $\boldsymbol{A} = 0$) is widely used. It can be forced through the addition of a penalty term (8). Then, the resulting discrete system equivalent to Eq. (29) is numerically stable and the solution is unique. However, the use of this gauge may have an adverse effect on the computation of flux density along iron–air interfaces unless a jump in the normal component of $\boldsymbol{A}$ is allowed along such interfaces (8). Surprisingly, the application of a gauge is unnecessary when using an iterative solver such as the incomplete Choleski conjugate gradient (*ICCG*) method. The accuracy of the magnetic field seems to be unaffected, and the stability is satisfactory with linear nodal elements. But when higher-order elements are used, the matrix of the system is seriously ill-conditioned, resulting in an excessively high number of ICCG iterations during the solution process.

Whitney Elements. The classical finite-element method is based on a node-oriented discretization. This is convenient for scalar or vector potentials because of their total continuity across interfaces between different media. But node elements are too rigid for vector fields, since they are generally a partially continuous with respect to either the tangential or normal component. A family of finite elements the Whitney elements, which provide adequate basis functions that naturally fit scalar and vector entities has been introduced during the last decade. Consider a tetrahedral section of a domain Ω four sets of simplices can be defined over the nodes, the edges, the facets, and the volumes (tetrahedra) of the mesh. Four related spaces W^p of finite elements are associated with them. The classical node elements form the space W^0 and relate to the nodes. The degrees of freedom are the nodal values. In the same way, edge elements (W^1), facet elements (W^2), and volume elements (W^3) are defined. Degrees of freedom are, respectively, the circulations along edges, the fluxes across facets, and volume integrals of the functions. Moreover, in the same way as any scalar function approximated in W^0 is continuous across the mesh, vector fields represented in W^1 and W^2 exhibit an implicit continuity of the tangential and normal components, respectively. Volume elements are not interesting for us and we will not discuss them further. An important feature of Whitney elements is the injective property that

exists between spaces:

$$\text{grad}\,(W^0) \subset W^1, \qquad \text{curl}(W^1) \subset W^2, \qquad \text{div}(W^2) \subset W^3$$

For instance, if the magnetic field $\boldsymbol{H}$ is approximated in terms of edge elements, its tangential continuity is naturally satisfied and its curl, the current density $\boldsymbol{J}$, lies in the space of facet elements so that its normal component is implicitly continuous.

The Magnetic Vector Potential Revisited. The use of edge elements to represent the magnetic vector potential has been introduced in order to avoid the numerical difficulties of nodal formulations. Thence, from the last section, it is clear that the continuity of the tangential component of $\boldsymbol{A}$ is automatically satisfied, without constraining the normal one, so that its divergence $\boldsymbol{B}$ presents the natural continuity of the normal component. The gauge $\boldsymbol{A}\cdot\boldsymbol{w} = 0$ seems suitable, where $\boldsymbol{w}$ is theoretically a vector field that does not form loops (9). In the present context, it consists of selecting a tree in the graph defined by the edges of the finite-element mesh and setting the degrees of freedom (tangential component of $\boldsymbol{A}$) corresponding to these edges to zero. The numerical accuracy as well as the rate of convergence depends on the choice of the tree. However, very slow convergence has been reported (10).

The alternative is the same as with nodal elements, that is, ungauging. Then conjugate gradients are again capable of solving the singular system resulting from Eq. (29) if the right-hand side is consistent, that is, the current density is exactly divergence free. This can be achieved by computing $\boldsymbol{J}$ as the curl of a current vector potential approached in the space of edge elements. Among the various classical magnetic vector potential formulations, this last one gives the best results while being numerically stable (10).

Magnetic Scalar Potentials. As an alternative to the vector potential, the most usual approach is in terms of scalar potentials owing to its economy with respect to the number of unknowns and its numerical stability. There are two types of scalar potentials according to the presence of current density as we shall show in the following.

The Total Scalar Potential ψ This potential is used for problems that do not involve the current density $\boldsymbol{J}$; then the magnetic field $\boldsymbol{H}$ is curl-free:

$$\text{curl}\,\boldsymbol{H} = \boldsymbol{0}$$

Therefore, $\boldsymbol{H}$ may be derived from a scalar potential function:

$$\boldsymbol{H} = -\,\text{grad}\,\psi$$

The use of Eqs. (2) and (3) leads to

$$\text{div}\,\mu\,\text{grad}\,\psi = \boldsymbol{0} \tag{30}$$

This is the nonhomogeneous Laplace equation. The potential $\psi$is often referred to as the total magnetic potential, since it is self-sufficient to describe the phenomenon.

The Reduced Scalar Potential. Most useful problems in magnetics involve either true current densities or fictitious ones in permanent magnets so that the notion of a scalar potential must be generalized. Therefore, Ampere's law (1) must be considered and $\boldsymbol{H}$ is not irrotational. Consider now the auxiliary problem in which all magnetic materials are removed; then the related field $\boldsymbol{H}_S$, is only due to the excitation current $\boldsymbol{J}$. This field can be obtained in a large variety of ways, for example, from the Biot–Savart law. However, although this is not the field of interest, it also verifies Ampere's law:

$$\text{curl}\,\boldsymbol{H}_s = \boldsymbol{J} \tag{31}$$

By subtraction, Eqs. (1) and (31) give

$$\text{curl}\,(\boldsymbol{H}-\boldsymbol{H}_s)=\boldsymbol{0}$$

so that the difference $\boldsymbol{H}-\boldsymbol{H}_{\text{s}}$, may be expressed in terms of a scalar potential ϕ. Then, the field $\boldsymbol{H}$ may be written as

$$\boldsymbol{H}=\boldsymbol{H}_s-\text{grad}\,\phi \tag{32}$$

Again, using Eq. (2), the following Poisson equation is obtained:

$$\text{div}\,\mu\,\text{grad}\,\phi=\text{div}\,\mu\,\boldsymbol{H}_s \tag{33}$$

Equation (32) shows that the function ϕ partially defines the field, therefore it is called the reduced scalar potential.

Two-Potential Formulation. The reduced potential is more general as stated before, but it leads to numerical instabilities in the computation of the magnetic field in the iron parts of the magnetostatic problems. Indeed, the field $\boldsymbol{H}$ in such highly permeable materials is considerably smaller than its value $\boldsymbol{H}_s$ in their absence. From Eq. (32), that amounts to saying that $\boldsymbol{H}_s$ and grad ϕ are of the same order of magnitude. Then the field $\boldsymbol{H}$ results from the cancellation of almost equal quantities, which renders the result very inaccurate. One possible cure for this problem is the use of both scalar potentials: the total potential of the iron parts (Ω_{i}), where there are generally no currents, and the reduced one of air and conductors (Ω_{a}). This two-potential formulation requires the explicit form of the continuity condition across the interface Γ between iron (μ) and nonmagnetic materials (μ_0). Those are expressed as

$$\begin{aligned}\mu\frac{\partial\psi}{\partial n}&=\mu_0\frac{\partial\phi}{\partial n}-\mu_0\boldsymbol{H}_s\cdot\boldsymbol{n}\\ \psi&=\phi-\int\boldsymbol{H}_s\,\boldsymbol{ds}\end{aligned} \tag{34}$$

where the last line integral is carried out along a path in the interface. As Eq. (33) is only valid in air space, it reduces to the Laplace equation, since $\mu=\mu_0$ and div $\mu_0\boldsymbol{H}_{\text{s}}=\text{div}\,\boldsymbol{B}_{\text{s}}=0$:

$$\nabla^2\phi=0 \tag{35}$$

The treatment of the ϕ–ψscheme with finite elements requires an integral formulation of Eqs. (30) and (35). Using the standard argument, Eqs. (30), (34), and (35) lead to the following weak form:

$$\int_{\Omega_i}\mu\,\text{grad}\,w\cdot\,\text{grad}\,\psi\,d\Omega+\int_{\Omega_a}\mu_0\,\text{grad}\,w\cdot\text{grad}\,\phi\,d\Omega-\oint_\Gamma\mu_0 w\boldsymbol{H}_s\cdot\boldsymbol{n}\,d\Gamma=0 \tag{36}$$

The second continuity condition in Eq. (34) must be added to complete the system.

There are some limitations to the use of scalar potentials. The most important occurs when multiply connected iron parts surround a coil so that the total scalar potential $\psi$is multivalued. Then some cutting surface is required in order to allow a discontinuity. This is rather awkward, as a general tractable algorithm to create cuts does not exist so far.

The Finite-Element Method–Boundary-Element Method Coupling. The finite-element method requires a volume discretization so that the number of unknowns becomes very large in three-dimensional analysis. Moreover, the necessity of meshing the surrounding air in the case of open problems requires the definition of a bounding box together with a further increase in the number of elements. Over the last two decades, the boundary-element method (*BEM*) has been developed as an interesting complementary finite-element-type technique for computational electromagnetics. In this method, only the boundary is divided into elements, and, in addition, an infinite region can be easily and economically analyzed. The main drawback is that it is not applicable to nonlinear media, which is a severe restriction in magnetostatic analysis. This leads to hybrid numerical schemes in which finite elements are used in the iron part of the problem, whereas boundary elements are used in the nonmagnetic regions. Such an FEM–BEM scheme may be applied to the two-potential formulation (11). The FEM–BEM coupling allows accurate computation of forces by using Maxwell's stress method. It is also very convenient for treating the movement of iron parts without remeshing.

The BEM method relies on the possibility of reducing the Laplace equation to a boundary integral formulation. Thus, Eq. (35) is equivalent to the expression

$$\frac{\alpha_P}{2\pi}\phi_P + \oint_\Gamma \left(\phi \frac{\partial w_P}{\partial n} - w_P \frac{\partial \phi}{\partial n}\right) d\Gamma = 0 \qquad (37)$$

where w_P is a singular weighting function (Green kernel) and α_P is the angle of the interior of Ω_i as viewed from the source point P. The value of α_P lies between 0 (outside the region) and 2π (inside the region). The contribution of an infinite boundary is simply zero so that open problems are easy to handle. It is clear that only Γ should be discretized into elements Γ_j so that Eq. (37) becomes

$$\frac{\alpha_P}{2\pi}\phi_P + \sum_{j=1}^{n} \int_{\Gamma_j} \left(\phi \frac{\partial w_P}{\partial n} - w_P \frac{\partial \phi}{\partial n}\right) d\Gamma = 0 \qquad (38)$$

Equation (38) has to be expressed at every node P of the boundary mesh, and an approximation (e.g., linear) for both ϕ and its normal derivative must be adopted. Then a set of algebraic equations of the following form is obtained:

$$\boldsymbol{H}\phi + \boldsymbol{G}\boldsymbol{q} = \boldsymbol{0} \qquad (39)$$

where $\boldsymbol{H}$ and $\boldsymbol{G}$ are square matrices and ϕ and $\boldsymbol{q}$ are the vectors of node potentials and node normal derivatives, respectively.

In the iron parts of the problem space, finite elements are used and the classical weak formulation of Eq. (30) is of concern. Discretization leads to a system of algebraic equations that must be merged with the system, Eq. (39), in order to describe the whole problem.

Mixed Formulations. Whitney elements have given rise to new formulations that are interesting alternatives for conventional formulations with scalar or vector potentials. The so-called mixed formulations are stated directly in terms of $\boldsymbol{H}$ or $\boldsymbol{B}$ fields with some auxiliary unknowns $\boldsymbol{A}$ or ϕ that have the meaning of dual potentials (12). For instance, the $\boldsymbol{H}$–$\boldsymbol{A}$ mixed formulation, or $\boldsymbol{H}$-conforming formulation, consists of finding $\boldsymbol{H}$ in W^1 and $\boldsymbol{A}$ in W^2 so that

$$\int_\Omega (\mu \boldsymbol{H}\cdot\boldsymbol{H}' - \boldsymbol{A}\cdot \operatorname{curl} \boldsymbol{H}')\, d\Omega = 0$$

$$\int_\Omega \operatorname{curl} \boldsymbol{H}\cdot\boldsymbol{J}' d\Omega = \int_\Omega \boldsymbol{J}\cdot\boldsymbol{J}' d\Omega$$

where $\boldsymbol{H}'$ and $\boldsymbol{J}'$ are test-vector fields chosen in W^1 and W^2, respectively. The complementary $\boldsymbol{B}$–ϕ formulation is symmetrically obtained.

Interesting features of mixed formulations are that they avoid cut problems in multiply connected domains and source-field computations. Moreover, gauging becomes implicit. The main drawback is the increase in the number of unknowns.

BIBLIOGRAPHY

1. C. W. Trowbridge Computing electromagnetic fields for research and industry since 1976: Major achievements and future trends, *IEEE Trans. Magn.*, **MAG-32**: 627–630, 1996.
2. Y. Saad *Iterative Methods for Sparse Linear Systems*, Boston: PWS, 1995.
3. G. Henneberger, *et al.* An accelerated Newton–Raphson method associated with the ICCG algorithm, *IEEE Trans. Magn.*, **MAG-26**: 709–711, 1990.
4. D. A. Lowther P. P. Silvester *Computer-Aided Design in Magnetics*, New York: Springer-Verlag, 1985.
5. J. L. Coulomb A methodology for the determination of global electromechanical quantities from finite element analysis and its application to the evaluation of magnetic forces, torques and stiffness, *IEEE Trans. Magn.*, **MAG-19**: 2514–2519, 1983.
6. J. Mizia *et al.* Finite element force calculation: comparison of methods for electric machines, *IEEE Trans. Magn.*, **MAG-24**: 447–450, 1988.
7. A. Razek *et al.* Conception of an air gap element for dynamic analysis of the electromagnetic field in electric motor, *IEEE Trans. Magn.*, **MAG-18**: 655–659, 1982.
8. K. Preis *et al.* Numerical analysis of 3D magnetostatic fields, *IEEE Trans. Magn.*, **MAG-27**: 3798–3803, 1991.
9. R. Albanese G. Rubinacci Magnetostatic field computations in terms of two component vector potentials, *Int. J. Num. Methods Eng.*, **MAG-29**: 515–532, 1990.
10. O. Biro K. Preis K. R. Richter On the use of the magnetic vector potential in the nodal and edge element analysis of 3D magnetostatic problems, *IEEE Trans. Magn.*, **MAG-32**: 651–654, 1996.
11. M. Ayoub *et al.* Numerical modeling of 3D magnetostatic saturated structures with a hybrid FEM-BEM technique, *IEEE Trans. Magn.*, **MAG-28**: 1052–1055, 1992.
12. A. Bossavit A rationale for edge elements in 3-D fields computations, *IEEE Trans. Magn.*, **MAG-24**: 74–79, 1988.

READING LIST

A. Bossavit *Computational Electromagnetism*, New York: Academic, 1998.

C. A. Brebbia (ed.) *Topics in Boundary Element Research*, **Vol. 6**, Berlin: Springer-Verlag, 1989.

C. A. Brebbia J. Dominguez *Boundary Elements, An Introductory Course*, 2nd ed., New York: Computational Mechanics Publication, 1992.

P. P. Silvester R. L. Ferrari *Finite Elements for Electrical Engineers*, Cambridge: Cambridge Univ. Press, 1983.

O. C. Zienkiewicz *The Finite Element Method*, Maidenhead: McGraw-Hill, 1977.

JACQUES LOBRY
Faculté Polytechnique de Mons
CHRISTIAN BROCHE
Faculté Polytechnique de Mons
JACQUES TRÉCAT
Faculté Polytechnique de Mons